

The spatial structure and dynamical state of the open cluster NGC 2112

Xinhua GAO,* ShouKun XU, and Lei XUE

School of Computer Science and Artificial Intelligence, Changzhou University, Changzhou 213164, China

*E-mail: xhgcczu@163.com

Received 2020 October 9; Accepted 2021 March 29

Abstract

This paper investigates the spatial structure and dynamical state of the old open cluster NGC 2112 based on likely cluster members from Gaia Early Data Release 3. Using the Density-Based Spatial Clustering of Applications with Noise (DBSCAN) algorithm, we find 1193 likely cluster members down to $G \sim 21$ mag within a radius of 1.5° from the cluster center. These likely cluster members can be divided into 865 core members and 328 border members by DBSCAN. We find that the core members are, on average, significantly brighter and more centrally concentrated than the border members. This suggests the existence of clear mass segregation within the cluster. We find that the outer regions of the cluster exhibit a slightly elongated shape, which may be caused by external tidal perturbations. We estimate a distance of $D = 1108 \pm 3$ pc for the cluster based on bright core members. We find that NGC 2112 has a cluster radius of $R_{\text{cl}} \sim 40'$ (~ 12.9 pc) and a core radius of $R_{\text{c}} \sim 4.8 \pm 0.2$ (~ 1.5 pc). This indicates that NGC 2112 has a central concentration parameter of $C = \log(R_{\text{cl}}/R_{\text{c}}) \sim 0.92$, which is significantly larger than previously thought. In addition, we estimate a total mass of $M_{\text{cl}} = 858 \pm 12 M_{\odot}$ and an initial mass of $M_{\text{ini}} = (2.2 \pm 0.5) \times 10^4 M_{\odot}$ for the cluster. This implies that NGC 2112 may have lost more than 90% of its initial mass. Based on the obtained distance and kinematical data, we also calculate the Galactic orbit of the cluster.

Key words: Hertzsprung–Russell and C–M diagrams—methods: statistical—open clusters and associations: individual (NGC 2112)—parallaxes—proper motions

1 Introduction

NGC 2112 ($l = 205.87$, $b = -12.62$) is a nearby open cluster with an age of ~ 1.8 Gyr (Carraro et al. 2008; Kharchenko et al. 2013; Haroon et al. 2017),¹ located at a distance of ~ 700 – 1000 pc (Richtler & Kaluzny 1989; Carraro et al. 2008; Kharchenko et al. 2013; Haroon et al. 2017) in the anti-center direction of the Galaxy. Our previous work shows that NGC 2112 may contain more than 700 member stars covering a wide range of star masses (Gao 2018b). This indicates that NGC 2112 is one of

the few rich and old open clusters in the solar neighborhood. NGC 2112 is therefore an important target for understanding the dynamical evolution of old open clusters. However, NGC 2112 suffers from heavy field star contamination (Richtler & Kaluzny 1989; Brown et al. 1996; Carraro et al. 2008). This makes it difficult to investigate the spatial structure and dynamical state of this cluster. Previous investigations led to discrepant results. Kharchenko et al. (2013) determined a core radius of 2.4 and a cluster radius of 37.2 for the cluster. Haroon, Ismail, and Elsanhoury (2017) estimated a core radius of 5.1 ± 0.5 and a limiting radius of 13.9 ± 1.3 for the cluster. They also

¹ (<https://webda.physics.muni.cz/>).

estimated a relaxation time of ~ 22 Myr for the cluster, which is much shorter than the cluster's age (~ 1.8 Gyr). This indicates that NGC 2112 is currently at an advanced state of dynamical evolution, and mass segregation should have occurred within the cluster. However, there is no clear evidence for the existence of mass segregation within NGC 2112. To investigate the spatial structure and dynamical state of NGC 2112, reliable cluster members are in great request.

For a long time it was not easy to segregate cluster members in NGC 2112 due to the lack of proper motions or radial velocities. Fortunately, the second Gaia data release (Gaia DR2) provides astrometric and photometric data for about 1.3 billion objects (Gaia Collaboration 2016, 2018), which are highly suitable for the studies of open clusters (Cantat-Gaudin et al. 2018; Gao 2018b, 2019b). Cantat-Gaudin et al. (2018) have determined 705 bright cluster members ($G < 18$ mag) for NGC 2112 using an unsupervised method (UPMASK). They also determined the distance and mean proper motion of the cluster. Unfortunately, their member list cannot be used to investigate the spatial structure and dynamical state of this old cluster due to the lack of faint members with $G > 18$ mag. This is because faint, low-mass members dominate the outer regions of this relaxed cluster (see subsection 3.1).

This paper aims to investigate the spatial structure and dynamical state of NGC 2112 based on Gaia Early Data Release 3 (Gaia EDR3). Gaia EDR3 provides improved astrometry and photometry for about 1.5 billion sources (Gaia Collaboration 2021). We will use the Density-Based Spatial Clustering of Applications with Noise (DBSCAN) (Ester et al. 1996) algorithm to identify reliable cluster members within a large field around the cluster. DBSCAN is an unsupervised clustering algorithm and has been used to identify cluster members of open clusters (Gao 2014; Bhattacharya et al. 2017; Castro-Ginard et al. 2018; Xu et al. 2019). The remainder of this paper is constructed as follows. In section 2 we identify cluster members using DBSCAN. In section 3 we investigate the spatial structure and dynamical state of NGC 2112. The last section summarizes the main conclusions of this work.

2 Data and method

2.1 Sample stars

Gaia EDR3 provides 5D astrometric parameters (positions, parallax, and proper motions) and magnitudes in three bands (G , BP , and RP) for about 1.5 billion sources (Gaia Collaboration 2021). In order to identify cluster members in NGC 2112, we must first select appropriate sample stars in Gaia EDR3. Based on Gaia DR2 data, Cantat-Gaudin et al.

(2018) have determined a mean parallax of $\varpi = 0.877 \pm 0.003$ mas and a mean proper motion of $(\mu_\alpha \cos \delta, \mu_\delta) = (-2.713 \pm 0.009, 4.270 \pm 0.009)$ mas yr $^{-1}$ for NGC 2112. Based on this information, we extract sample stars using the following criteria: (1) the stars must lie within a radius of 1.5° from the cluster center; (2) the stars must have parallaxes between 0.4 and 2.0 mas; (3) the stars must lie in the proper motion range of $-6 < \mu_\alpha \cos \delta < 0$ and $0 < \mu_\delta < 6$ mas yr $^{-1}$; and (4) the stars must have magnitudes in three bands. The selection radius (1.5°) is about 6.5 times as large as the limiting radius of the cluster (Haroon et al. 2017). This allows us to identify cluster members up to ~ 25 pc from the cluster center, assuming a cluster distance of 940 pc (Carraro et al. 2008). The parallax and proper motion criteria allow us to reject as many field stars as possible. This will greatly enhance the clustering performances of DBSCAN. Finally, we obtain 9135 sample stars, each of which has astrometric and photometric data.

2.2 Method

Based on Gaia DR2 data, we have obtained 740 likely members within a $20'$ radius of NGC 2112 using a Gaussian Mixture Model (GMM) clustering method (Gao 2018b). However, the GMM method cannot identify more cluster members within a larger field around the cluster, because it is model-dependent and sensitive to sample stars (Gao 2018a). As a model-independent method, DBSCAN is able to discover clusters with arbitrary shape in large data sets based on two input parameters: the search radius (Eps) and the minimum number of points ($MinPts$) within Eps (Ester et al. 1996). Another advantage of DBSCAN is that no prior knowledge about clusters is required (Ester et al. 1996). This allows us to identify cluster members in NGC 2112 from a large number of sample stars in a more robust manner. DBSCAN can divide a given set of data points into three types: core points, border points, and noise points (Ester et al. 1996), and the former two have higher average densities than the latter one. In this paper, the core points and border points are regarded as likely cluster members, and the noise points are considered as field stars.

To enhance the clustering performances of DBSCAN, we first normalize the original data in each dimension using the following formula:

$$x'_i = \frac{x_i - \text{Min}(X)}{\text{Max}(X) - \text{Min}(X)}, \quad (1)$$

where $X = (x_1, x_2, x_3, \dots, x_n)$ is the original data set, and x'_i is the i th normalized data point. $\text{Min}(X)$ and $\text{Max}(X)$ indicate the minimum and maximum values of the original data set, respectively. This allows us to rescale the

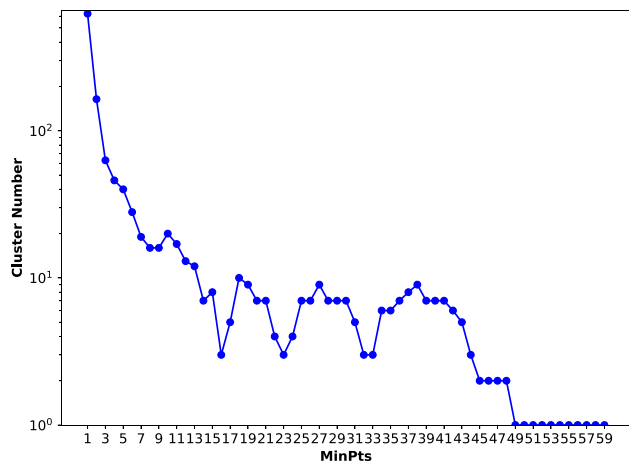


Fig. 1. Cluster number as a function of $MinPts$ for the sample stars in the field of NGC 2112. (Color online)

original data to the specified range $[0, 1]$. After doing this, principle-component analysis (PCA) is used to find the most informative components in the 5D normalized data. This step helps to decrease the noise in our data set (Gao 2020). We find that the most informative four components contain about 88% of the total variance. In the 4D PC space, we perform DBSCAN clustering for different values of $MinPts$ with an increment of $\Delta MinPts = 1$ keeping a

constant search radius of $Eps = 0.1$. We adopt this search radius ($Eps = 0.1$) because our sample is relatively sparse in the 4D PC space. For each value of $MinPts$, we count the number of the clusters discovered by DBSCAN. In general, the cluster number decreases with the increment of $MinPts$ (see figure 1). We find that only one cluster (NGC 2112) can be detected if $MinPts$ is greater than or equal to 49. In this paper we identify cluster members of NGC 2112 based on the input parameters ($Eps, MinPts$) = (0.1, 49).

2.3 Likely cluster members

Based on the appropriate input parameters, DBSCAN can find 865 core members and 328 border members within a radius of 1.5° from the cluster center (see table 1). The core members can be regarded as the most probable cluster members, because they are identified as core points by DBSCAN. The border members, which are identified as border points, are more likely to be cluster members than field stars (noise points). Figure 2 shows the spatial positions of the 1193 likely cluster members. We find that the core members are significantly more centrally concentrated than the border members. It is found that the outer regions of NGC 2112 exhibit a slightly elongated shape, which roughly distributes along the cluster orbit (see figure 11

Table 1. Fundamental information of the 1193 likely cluster members.*

Gaia-ID	RA ($^\circ$)	Dec ($^\circ$)	Member type
3218732127521861888	088.30468054211	+00.18586529376	c
3218823932448482688	088.68802088019	+00.37380479647	c
3218866989495548032	088.76772254203	+00.65760431894	c
3218826960400252544	088.49831787561	+00.23835846031	c
3218825616074916864	088.43863822057	+00.23247747270	c
3218890693419688064	088.34494514545	+00.53623166763	c
3218834107225970560	088.61701910969	+00.35363378291	c
3218829533085109120	088.34092549902	+00.27164198116	c
3218840115885472640	088.61322759691	+00.46532559350	c
3218881794247401600	088.31400053562	+00.50637499737	c
3218878500007817856	088.27948601114	+00.39339178325	c
3218881691168159872	088.30318773897	+00.49066514811	c
3218877774157809792	088.22340534758	+00.33778685333	b
3218844135975109504	088.95071843277	+00.41202641411	b
3218932204278736256	088.40700297689	+00.85495205760	b
3218912202616166656	088.23686547811	+00.85309550031	b
3218596990671530240	089.00115992956	-00.21030950534	b
3218838982013249280	088.45879607244	+00.41786024252	b
3218899665606371712	087.99614244458	+00.56053495733	b
3218735215603249408	088.30757360781	+00.21335978338	b
...

*This table contains Gaia EDR3 identifiers, positions and member types for the 1193 likely cluster members identified by DBSCAN. Only a portion of this table is shown here to demonstrate its form and content; a machine-readable version of the full table is available from the authors on request. The cluster members can be divided into two types: core members (c) and border members (b).

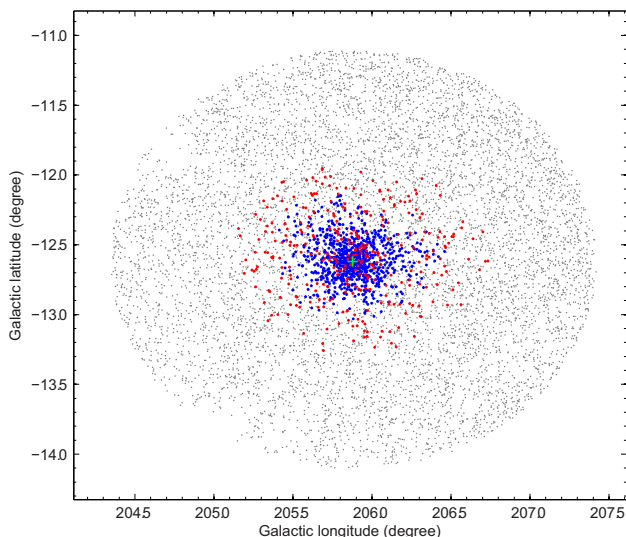


Fig. 2. Positions of the 1193 likely cluster members in NGC 2112. The blue and red dots indicate the core and border members, respectively, and the gray dots indicate the field stars (noise points). The green plus is the new estimate (205.878, -12.619) for the cluster center based on the Mean Shift method. (Color online)

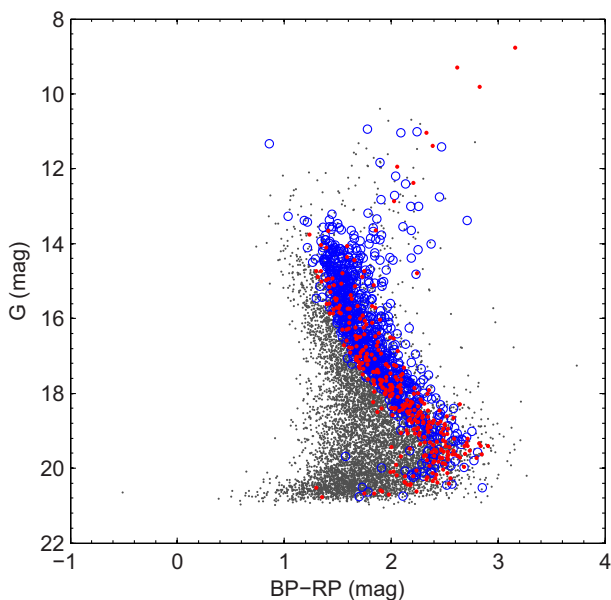


Fig. 3. CMDs of the core members (blue circles), border members (red dots), and field stars (gray dots). (Color online)

in subsection 3.3). Based on the 1193 likely members, we estimate the position of the cluster center using the Mean Shift method (Comaniciu & Meer 2002), which can find the central position for the densest region in the cluster (see figure 2). Our results (205.878, -12.619) are consistent with those obtained by Cantat-Gaudin et al. (2018). Figures 3 and 4 show the color-magnitude diagrams (CMDs) and proper motions of the 1193 likely cluster members, respectively. Compared with our previous work

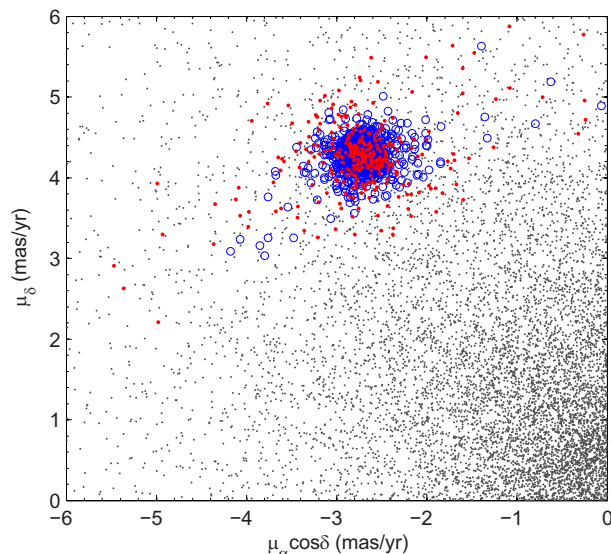


Fig. 4. Proper motions of the core members (blue circles), border members (red dots), and field stars (gray dots). (Color online)

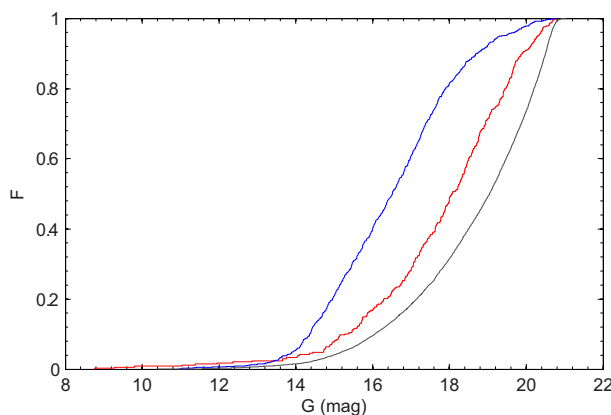


Fig. 5. CDFs of the core members (blue curve), border members (red curve), and field stars (gray curve). (Color online)

(Gao 2018b), the present work identifies more cluster members within a larger cluster-centric radius of 1.5° . This helps to improve our understanding of the spatial structure and dynamical state of the cluster.

3 Fundamental properties of the cluster

3.1 Spatial structure and dynamical state

Based on DBSCAN, we have obtained 1193 likely cluster members, including 865 core members and 328 border members. The CMDs in figure 3 show that there is a clear lack of bright stars ($G < 15$ mag) for the border members as compared to the core members. The cumulative distribution functions (CDFs) show that the core members are, on average, brighter than the border members (see figure 5). The CMDs and CDFs indicate that clear mass

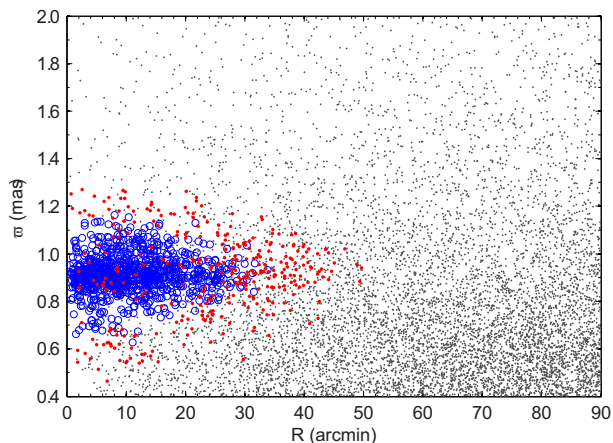


Fig. 6. Distance to the cluster center (R) as a function of the parallax (ϖ) for the likely cluster members. The blue circles and red dots indicate the core members and border members, respectively, and the gray dots indicate field stars. (Color online)

segregation has occurred within the cluster. Mass segregation is expected to occur in relatively old clusters, which have enough time to reach a state of energy equipartition (Binney & Tremaine 1987). The typical relaxation time of an open cluster with 1000 members is less than 0.1 Gyr (Bonatto & Bica 2003; Chen et al. 2004). Even for a rich cluster with 10000 members, the relaxation time is shorter than 1 Gyr (Bonatto & Bica 2003). This indicates that the observed mass segregation within NGC 2112 is the result of dynamical relaxation. The elongated shape of NGC 2112 (see figure 2) may be the result of external tidal perturbations (Chen et al. 2004; Sánchez & Alfaro 2009; Vicente et al. 2016).

We plot the distance to the cluster center as a function of the parallax for the likely cluster members (see figure 6). We find that the border members extend up to distances of $\sim 50'$ from the cluster center. This value is significantly larger than the radial extent ($\sim 30'$) of the core members (see figure 6). It is reasonable to adopt a mean cluster radius of $R_{\text{cl}} \sim 40'$ for NGC 2112. This value is about 2.9 times the result ($\sim 13'.9 \pm 1'.3$) derived by Haroon et al. (2017). The likely members also allow us to estimate the core radius (R_c) for the cluster based on the King model (King 1962) as

$$\rho(r) = f_b + \frac{f_0}{1 + (r/R_c)^2}, \quad (2)$$

where $\rho(r)$ denotes the star surface density at the distance r from the cluster center, and f_b and f_0 are the background density and cluster central density, respectively. We obtain the radial density profile (RDP) for the core and border members within $40'$ of the cluster center. Fitting of the King model to the RDP yields a core radius of $R_c = 4'.8 \pm 0'.2$ (see figure 7), which is consistent with the result

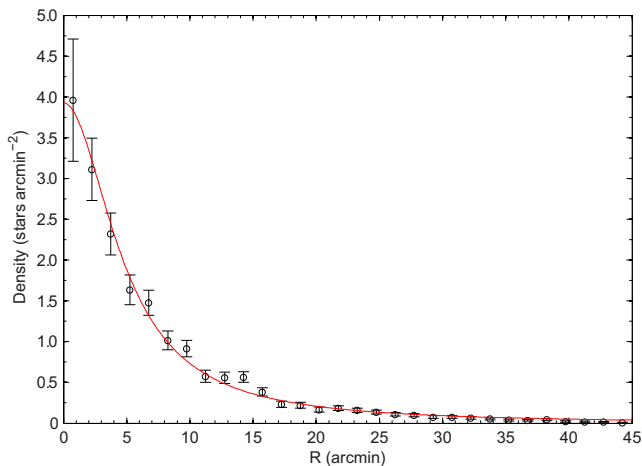


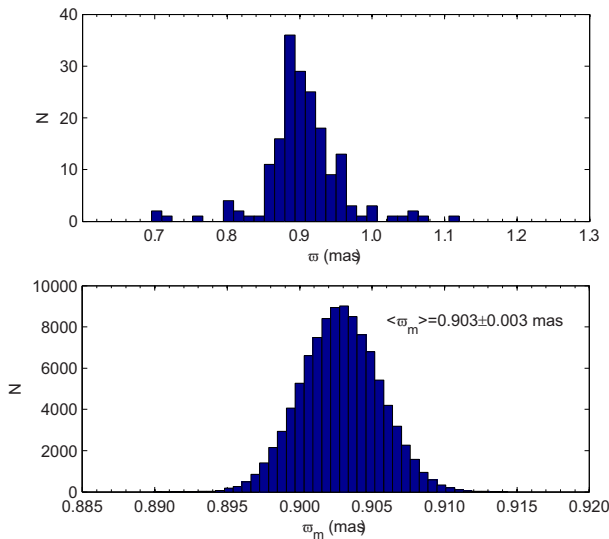
Fig. 7. RDP of the likely cluster members within $40'$ of the cluster center. The error bars denote the 1σ Poisson errors, and the solid line is the King profile (King 1962).

($5'.1 \pm 0'.5$) derived by Haroon et al. (2017) within the 1-sigma uncertainty interval. The central concentration parameter (Peterson & King 1975) of the cluster is determined to be $C = \log(R_{\text{cl}}/R_c) \sim 0.92$, which is significantly larger than that (0.44) of Haroon et al. (2017). In table 2, we list 21 cluster members with Gaia radial velocities (RVs). We determined a mean RV of $\bar{V}_r = 31.2 \pm 0.4 \text{ km s}^{-1}$ for the 14 core members based on 100000 Monte Carlo simulations (Gao 2019a). This value is in good agreement with the result ($30.9 \pm 0.4 \text{ km s}^{-1}$) reported by Carraro et al. (2008) within the 1-sigma uncertainty interval. Among the 21 members, star #3219687706206179328 is located at $\sim 36'$ from the cluster center. It has an RV of $30.42 \pm 0.27 \text{ km s}^{-1}$, which agrees well with the mean RV of the cluster. It therefore provides a lower limit of $\sim 36'$ for the cluster radius. Star #3218603381582833280 is likely not a cluster member, because it has an RV of $97.72 \pm 3.77 \text{ km s}^{-1}$.

A mean parallax of NGC 2112 is also estimated based on the 182 bright core members with $G < 15 \text{ mag}$, because these stars have relatively precise Gaia parallaxes. Using the same Monte-Carlo method, we obtain a mean parallax of $\bar{\varpi} = 0.903 \pm 0.003 \text{ mas}$ (see figure 8), which is slightly larger than that ($0.877 \pm 0.003 \text{ mas}$) determined by Cantat-Gaudin et al. (2018). It has been shown that Gaia EDR3 parallaxes have a relatively low zero-point offset (Stassun & Torres 2021; Zinn 2021). Based on the mean parallax, we determine the cluster distance to be $D = 1108 \pm 3 \text{ pc}$ without taking into account the zero-point offset in the parallaxes. Our result is consistent with the value ($940 \pm 70 \text{ pc}$) derived by Carraro et al. (2008) within the 3-sigma uncertainty interval. Our result is also consistent with the distance ($\sim 994\text{--}1241 \text{ pc}$) in Cantat-Gaudin et al. (2018). Using the same method and sample stars,

Table 2. Gaia radial velocities for 21 likely cluster members.

Gaia-ID	RA (°)	Dec (°)	RV (km s ⁻¹)	eRV (km s ⁻¹)	Member type
3218829365581985920	088.31681556131	+00.25207322643	30.41	0.71	c
3218837130882723200	088.59628970006	+00.44847703987	33.97	10.65	c
3218833587534160128	088.58767479226	+00.33012073216	31.27	0.29	c
3218888876648697088	088.50080603233	+00.56974337902	29.44	1.04	c
3218878396928610560	088.26405610290	+00.38212799801	31.01	4.99	c
3218840257618901376	088.62827278511	+00.47941295313	31.26	0.21	c
3218884852263788032	088.30984506660	+00.53704815778	31.22	0.72	c
3218880561592085888	088.33809888119	+00.44399388464	29.05	1.20	c
3218832629757236480	088.38902990481	+00.38158589496	32.58	2.06	c
3218833076433648256	088.43238299429	+00.39913280833	30.67	8.50	c
3218838230394388608	088.47206007136	+00.41050227665	33.92	1.12	c
3218831289727287040	088.41914134009	+00.30889400587	33.93	3.34	c
3218886883783895680	088.45270754081	+00.50743424275	33.12	4.69	c
3218812494950559488	088.55617106241	+00.17143093679	30.93	0.62	c
3218899489512322304	087.99482626155	+00.53651335731	30.75	0.89	b
3218603381582833280	089.00858332262	-00.06505801497	97.72	3.77	b
3219654750920489728	088.01201646178	+00.76168719184	30.83	0.37	b
3218837886797001344	088.51328613013	+00.38335795813	29.42	0.73	b
3218849083776896512	088.95817518276	+00.48904019423	30.68	0.31	b
3219687706206179328	088.30415064041	+00.98628976784	30.42	0.27	b
3218936082633687424	088.24790630648	+00.89569729015	30.38	0.34	b


Fig. 8. Gaia parallaxes of the 182 core members (top panel) and Monte Carlo simulations (100000 times) of their median parallax (bottom panel). (Color online)

we estimate a mean proper motion of $(-2.715 \pm 0.005, 4.275 \pm 0.005)$ mas yr⁻¹, which agrees well with the result obtained by Cantat-Gaudin et al. (2018).

Based on the mean radius R_{cl} of the cluster (40' or 12.9 pc), we estimate the total mass M_{cl} enclosed in this radius using the following formula (King 1962):

$$M_{\text{cl}} = \frac{4A(A-B)}{G} R_{\text{cl}}^3, \quad (3)$$

where G is the gravitational constant, and A and B indicate the Oort constants. In this paper we adopt $A = 15.3 \pm 0.4$ km s⁻¹ kpc⁻¹ and $B = -11.9 \pm 0.4$ km s⁻¹ kpc⁻¹ (Bovy 2017). The total mass of the cluster is determined to be $M_{\text{cl}} = 858 \pm 12 M_{\odot}$, which is somewhat higher than that ($\sim 641 M_{\odot}$) obtained by Haroon et al. (2017). The disruption time of a cluster with mass $10^4 M_{\odot}$ is about 1.3 ± 0.5 Gyr (Lamers et al. 2005), which is slightly shorter than the current age of NGC 2112 (~ 1.8 Gyr). This indicates that NGC 2112 should have a high initial mass exceeding $10^4 M_{\odot}$.

3.2 Initial mass

The initial mass M_{ini} of the cluster can be estimated using the method proposed by Lamers et al. (2005). This analytic method has been used to estimate the initial masses of the open clusters NGC 6791 (Dalessandro et al. 2015) and Ruprecht 147 (Yeh et al. 2019). The initial mass of the cluster can be written as (Yeh et al. 2019)

$$M_{\text{ini}} = \left[\left(\frac{M_c}{M_{\odot}} \right)^{\gamma} + \frac{\gamma t}{t_0} \right]^{1/\gamma} [1 - q_{\text{ev}}(t)]^{-1}, \quad (4)$$

where M_c and t are the present-day mass and age of the cluster, respectively, and $q_{\text{ev}}(t)$ is the mass loss due to stellar evolution. Carraro et al. (2008) determined a slightly super-solar abundance ($[\text{Fe}/\text{H}] \sim 0.16$) for NGC 2112. According

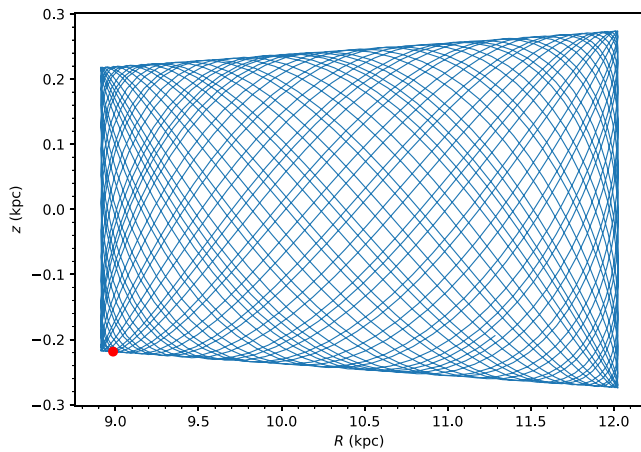


Fig. 9. 2D side view of the cluster's orbit; the red dot is the current position of the cluster. (Color online)

to the values in Lamers et al. (2005), the function $q_{ev}(t)$ is written as

$$\log_{10} q_{ev}(t) = (\log_{10} t - 7.0)^{0.255} - 1.805. \quad (5)$$

To estimate the initial mass, we adopt $\gamma = 0.62$, $t_0 = 3.3$ (Yeh et al. 2019), $M_c = 858 \pm 12 M_\odot$, and $t = 1.8 \pm 0.3$ Gyr (Carraro et al. 2008) in this work. Finally, we obtain an estimate of $M_{ini} = (2.2 \pm 0.5) \times 10^4 M_\odot$ by taking into account the uncertainties of the parameters. This implies that NGC 2112 may have lost more than 90% of its initial mass.

3.3 Galactic orbit of the cluster

The obtained distance, proper motions and radial velocity allow us to calculate the orbit of NGC 2112. In this paper, we determine the orbit parameters of the cluster using the galpy python package (Bovy 2015). To do this, the MWPotential2014 model is adopted to describe the Milky Way's gravitational potential (Bovy 2015). The solar distance to the Galactic center and the circular velocity at the Sun are set to $R_\odot = 8.0$ kpc and $V_{LSR} = 220$ km s⁻¹, respectively (Bovy & Tremaine 2012). We adopt the solar motion $(U_\odot, V_\odot, W_\odot) = (11.1, 12.24, 7.25)$ km s⁻¹ derived by Schönrich et al. (2010). The orbit is followed backwards for a time interval of 6 Gyr, which is larger than the age of the cluster. The apogalactic (R_a) and perigalactic (R_p) distances are determined to be 12.028 and 8.913 kpc, respectively. Figure 9 shows that NGC 2112 has a confined box-type orbit ($8.913 \leq R \leq 12.028$ kpc). We find that the cluster has an orbit eccentricity of $e \sim 0.149$ (see figure 10), and its maximum distance from the Galactic plane is about $Z_{max} \sim 0.274$ kpc (see figure 9). NGC 2112 is currently at its maximum height on the Galactic plane, because the Z-component of its velocity is close to zero (~ -1.5 km s⁻¹). The orbit parameters suggest that NGC 2112 is a typical

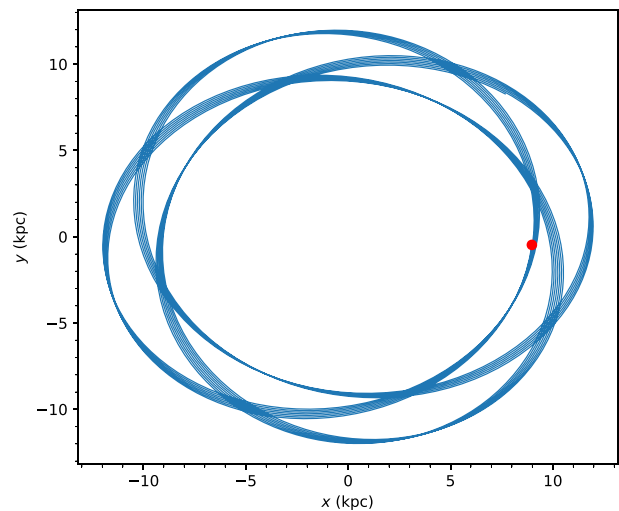


Fig. 10. 2D top view of the cluster's orbit; the red dot is the current position of the cluster. (Color online)

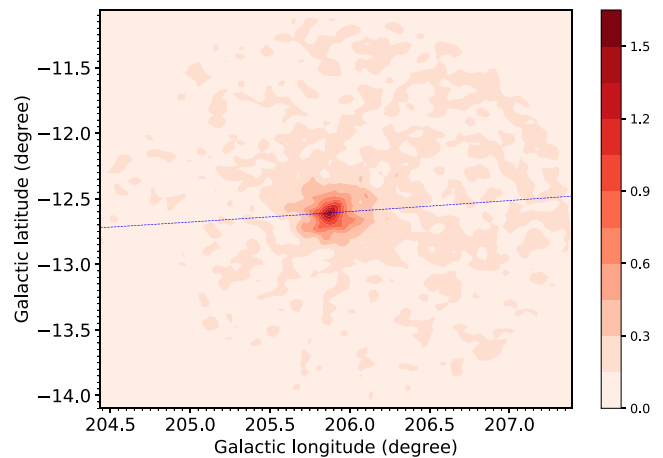


Fig. 11. 2D density map of the sample stars; the blue dashed line is the projected orbit. (Color online)

thin-disc cluster orbiting well outside the solar circle. We also plot the projected cluster orbit and 2D density map of the sample stars (see figure 11). NGC 2112 appears to have a clear core–halo structure, and its elongated shape roughly distributes along the cluster orbit.

4 Conclusions and discussions

NGC 2112 is an important target for studying the dynamical evolution of open clusters in the solar neighborhood. This paper investigates the spatial structure and dynamical state of NGC 2112 using Gaia EDR3 data. For this purpose, we identify 1193 likely cluster members within 1.5° of the cluster using DBSCAN clustering. We confirm that DBSCAN can find reliable cluster members in noisy environments (heavy field star contamination). Therefore, our method, in principle, can also be used to investigate other open clusters.

We find that clear mass segregation has occurred within the cluster due to dynamical relaxation. We also find that NGC 2112 has an extended halo and exhibits a slightly elongated shape (see figure 11), which may be caused by external tidal perturbations. The distance of the cluster is estimated to be 1108 ± 3 pc, which is consistent with the photometric distance obtained by Carraro et al. (2008). We determine a mean cluster radius of $40'$ (~ 12.9 pc) and a core radius of 4.8 ± 0.2 (~ 1.5 pc) for NGC 2112. The central concentration parameter of the cluster is determined to be ~ 0.92 , indicating that NGC 2112 is at an advanced state of dynamical evolution. We estimate a total mass of $858 \pm 12 M_{\odot}$ within the cluster radius. However, it is probably a lower limit, because the cluster radius may be underestimated (see figure 6) and the total mass is sensitive to the cluster radius (see equation 3). We find that NGC 2112 may have an initial mass of $(2.2 \pm 0.5) \times 10^4 M_{\odot}$. This indicates that NGC 2112 may have lost more than 90% of its initial mass. The high initial mass and compact spatial structure may explain why NGC 2112 has survived to its present age (~ 1.8 Gyr). We calculate the Galactic orbit of NGC 2112 based on the obtained distance and kinematical data. The orbit parameters show that NGC 2112 belongs to the thin-disc population.

Conflict of Interest

The authors declared that they have no conflicts of interest to this work.

Acknowledgments

We would like to thank the anonymous referee for his/her careful reading and helpful comments. This research was supported by the Foundation of Changzhou University (Grant No. GJY18020008). This work has made use of data from the European Space Agency (ESA) mission Gaia (<https://www.cosmos.esa.int/gaia>), processed by the Gaia Data Processing and Analysis Consortium (DPAC, <https://www.cosmos.esa.int/web/gaia/dpac/consortium>). Funding for the DPAC has been provided by national institutions, in particular the institutions participating in the Gaia Multilateral Agreement. This research has made use of the VizieR catalog access tool, CDS, Strasbourg, France.

References

Bhattacharya, S., Mahulkar, V., Pandaokar, S., & Singh, P. K. 2017, *Astron. Comput.*, 18, 1

- Binney, J., & Tremaine, S. 1987, *Galactic Dynamics*, 2nd ed. (Princeton: Princeton University Press)
- Bonatto, C., & Bica, E. 2003, *A&A*, 405, 525
- Bovy, J. 2015, *ApJS*, 216, 29
- Bovy, J. 2017, *MNRAS*, 468, L63
- Bovy, J., & Tremaine, S. 2012, *ApJ*, 756, 89
- Brown, J. A., Wallerstein, G., Geisler, D., & Oke, J. B. 1996, *AJ*, 112, 1551
- Cantat-Gaudin, T., et al. 2018, *A&A*, 618, A93
- Carraro, G., Villanova, S., Demarque, P., Moni Bidin, C., & McSwain, M. V. 2008, *MNRAS*, 386, 1625
- Castro-Ginard, A., Jordi, C., Luri, X., Julbe, F., Morvan, M., Balaguer-Núñez, L., & Cantat-Gaudin, T. 2018, *A&A*, 618, A59
- Chen, W. P., Chen, C. W., & Shu, C. G. 2004, *AJ*, 128, 2306
- Comaniciu, D., & Meer, P. 2002, *IEEE Trans. Pattern Anal. Machine Intell.*, 24, 603
- Dalessandro, E., Mocchi, P., Carraro, G., Jilková, L., & Moitinho, A. 2015, *MNRAS*, 449, 1811
- Ester, M., Kriegel, H.-P., Sander, J., & Xiaowei, X. 1996, in *Proc. Second Int. Conf. Knowledge Discovery in Databases and Data Mining* (Palo Alto: Association for the Advancement of Artificial Intelligence), 226
- Gaia Collaboration 2016, *A&A*, 595, A1
- Gaia Collaboration 2018, *A&A*, 616, A1
- Gaia Collaboration 2021, *A&A*, 649, A1
- Gao, X. 2018a, *ApJ*, 869, 9
- Gao, X. 2020, *PASJ*, 72, 47
- Gao, X.-H. 2014, *Res. Astron. Astrophys.*, 14, 159
- Gao, X.-H. 2018b, *PASP*, 130, 124101
- Gao, X.-H. 2019a, *PASP*, 131, 044101
- Gao, X.-H. 2019b, *PASJ*, 71, 62
- Haroon, A. A., Ismail, H. A., & Elsanhoury, W. H. 2017, *Astrophys.*, 60, 173
- Kharchenko, N. V., Piskunov, A. E., Schilbach, E., Röser, S., & Scholz, R.-D. 2013, *A&A*, 558, A53
- King, I. 1962, *AJ*, 67, 471
- Lamers, H. J. G. L. M., Gieles, M., Bastian, N., Baumgardt, H., Kharchenko, N. V., & Portegies Zwart, S. 2005, *A&A*, 441, 117
- Peterson, C. J., & King, I. R. 1975, *AJ*, 80, 427
- Richtler, T., & Kaluzny, J. 1989, *A&AS*, 81, 225
- Sánchez, N., & Alfaro, E. J. 2009, *ApJ*, 696, 2086
- Schönrich, R., Binney, J., & Dehnen, W. 2010, *MNRAS*, 403, 1829
- Stassun, K. G., & Torres, G. 2021, *ApJ*, 907, L33
- Vicente, B., Sánchez, N., & Alfaro, E. J. 2016, *MNRAS*, 461, 2519
- Xu, S.-k., Wang, C., Zhuang, L.-h., & Gao, X.-h. 2019, *Chin. Astron. Astrophys.*, 43, 225
- Yeh, F. C., Carraro, G., Montalto, M., & Seleznev, A. F. 2019, *AJ*, 157, 115
- Zinn, J. C. 2021, *AJ*, 161, 214